

PoreNet: CNN-based Pore Descriptor for High-resolution Fingerprint Recognition

Vijay Anand, *Student Member, IEEE*, and Vivek Kanhangad, *Senior Member, IEEE*

Abstract—With the development of high-resolution fingerprint scanners, high-resolution fingerprint-based biometric recognition has received increasing attention in recent years. This letter presents a pore feature-based approach for biometric recognition. Our approach employs a convolutional neural network (CNN) model, DeepResPore, to detect pores in the input fingerprint image. Thereafter, a CNN-based descriptor is computed for a patch around each detected pore. Specifically, we have designed a residual learning-based CNN, referred to as PoreNet that learns distinctive feature representation from pore patches. For verification, the match score is generated by comparing pore descriptors obtained from a pair of fingerprint images in bi-directional manner using the Euclidean distance. The proposed approach for high-resolution fingerprint recognition achieves 2.56% and 0.57% equal error rates (EERs) on partial (DBI) and complete (DBII) fingerprints of the benchmark PolyU HRF dataset. Most importantly, it achieves lower FMR1000 and FMR10000 values than the current state-of-the-art approach on both the datasets.

Index Terms—High-resolution fingerprints, fingerprint recognition, pore descriptor, Convolutional neural network.

I. INTRODUCTION

FINGERPRINT is one of the most widely explored biometric traits, mainly due its distinctiveness and permanence [1]. The features extracted from a fingerprint image are broadly classified into level 1, level 2 and level 3 features. Level 1 features, which include global ridge orientation, are commonly used for fingerprint classification. Level 2 fingerprint features include finer details such as ridge endings and ridge bifurcations, which are collectively called minutiae [1]. Level 3 fingerprint features, on the other hand, include very fine details such as pores, incipient ridges, dots, and ridge contours. Level 1 and level 2 features can be observed in 500 dpi fingerprint images, while level 3 features are generally observable in fingerprint images having a resolution greater than 800 dpi [2].

Commercially available automated fingerprint recognition systems (AFRS) and a majority of the methods reported in the literature employ level 1 and level 2 features. However, with the advent of high-resolution fingerprint sensors, there has been a focus shift and several methods that employ level 3 features have been developed for fingerprint recognition. In addition to enhancing the recognition performance, level 3 features provide higher level of security, as they are difficult to forge. Further, the level 3 features have also been included in the extended feature set for fingerprint recognition [3].

Over the last few years, there has been growing interest in level 3 fingerprint features, especially the pores and several methods have been proposed for pore feature based automated fingerprint recognition [4]–[16]. The earliest works [4]–[7] employed skeletonization-based approach for pore detection which is suitable only for very high-resolution (~ 2000 dpi) fingerprint images and is not robust against fingerprint degradation caused by skin conditions. In order to circumvent these challenges, Jain *et al.* [8] presented a hierarchical fingerprint recognition approach which utilizes features from all the three levels. For matching level 3 features, fingerprints are first matched using minutiae and then level 3 features are extracted in the neighbourhood of the matched minutiae points. Finally, the extracted level 3 features are matched using iterative closest point (ICP) algorithm. Later on, Zhao *et al.* [9] proposed a direct pore matching approach. Pores are extracted by employing adaptive pore filtering methodology [17]. For each pore, a descriptor is formed by considering the pixels' intensity in the neighbourhood of the pore pixel. Initial correspondence is established by calculating dot product between the descriptor vectors of two pore sets. Final refinement is then achieved by employing random sample consensus (RANSAC) algorithm. Authors have also shown that pores are effective for recognition using partial fingerprint images, which may not contain sufficient level-2 features [10], [11]. Liu *et al.* [12] proposed an improved direct pore matching approach. Firstly, pores are represented by a local descriptor as in [9]. Then coarse correspondence is obtained by using sparse representation coefficients of the pores. Finally, weighted RANSAC (WRANSAC) [18] algorithm is employed to refine the coarse correspondence. Authors in [13] extended the work in [12] by using tangent distance and sparse representation-based matching to compare the pores of reference and probe fingerprint images. The final refinement of the initial correspondences is obtained by employing WRANSAC.

Recently, Lemes *et al.* [14] proposed a dynamic pore filtering approach which is adaptive to the pore size variations and involves less computational cost. Segundo and Lemes [15] improved the dynamic pore filtering approach in [14] by considering the average ridge width in place of average valley width to obtain global and local radii which are used in the same manner as in [14]. Most recently, Dahia and Segundo [19] presented an approach to generate pore annotation by aligning the fingerprint images in the training set and then learned the descriptor for each of the pore patches by employing an existing CNN-based patch matching model, HardNet [20]. Authors in [21] proposed two-step method to compare pores present in fingerprint images. Firstly, fingerprint images

V. Anand and V. Kanhangad are with the Discipline of Electrical Engineering, Indian Institute of Technology Indore, Indore 453552, India e-mail: phd1401202011@iiti.ac.in (V. Anand), kvivek@iiti.ac.in (V. Kanhangad).

are aligned using a data-driven descending algorithm. The alignment is obtained by using the fingerprint ridges and orientation field. Once the fingerprint images are aligned, the pores present in the overlapping area between the two fingerprint images are then matched using graph comparison method.

It can be observed from the literature that the performance of the existing high-resolution AFRS can be improved by combining better level 3 feature detection technique with robust point matching technique. The objective of this work is to advance the state-of-the-art in high-resolution fingerprint recognition using pore-descriptor based fingerprint matching. Specifically, we have leveraged on CNN-based deep embedding learning, which has been employed for various computer vision problems [22]–[24]. However, the application of CNN in biometrics is still very limited especially for fingerprint recognition. The main reason could be the unavailability of the large labeled dataset required for training the CNN. The major contributions of this paper are as follows: firstly, we have developed an automated approach to generate labels for the common pores present among different impressions of the same finger of the training images. Secondly, we have designed a residual learning-based convolutional neural network, referred to as PoreNet, for learning the distinctive feature representation of pore patches in high-resolution fingerprint images.

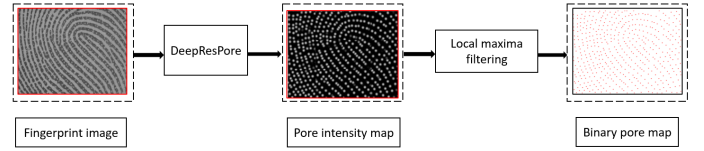
The rest of the paper is organized as follows: Section II presents a brief introduction of the proposed methodology followed by a detailed description of the pore label generation approach and the pore descriptor learning approach. Experimental results and discussion are presented in Section III. Finally, the concluding remarks are presented in Section IV.

II. PROPOSED METHOD

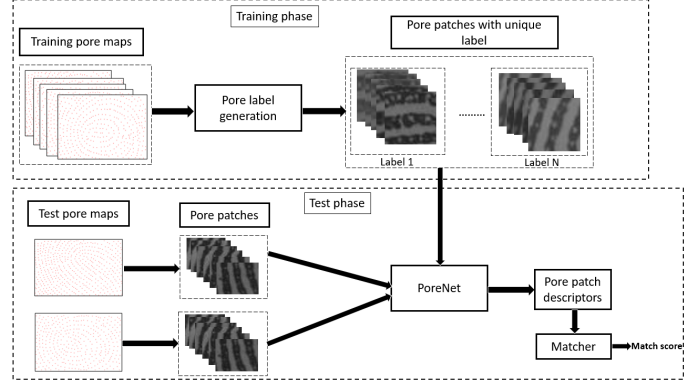
In this letter, we present a pore feature-based methodology for high-resolution fingerprint recognition. In the first stage, pores are detected in a high-resolution fingerprint image by employing DeepResPore [25] which generates a pore intensity map. The pore intensity map is processed further to obtain a binary pore map. In second stage, pore descriptor is learned by employing a customized deep residual learning-based CNN model referred to as PoreNet. PoreNet takes pore patches as input and converts them to the corresponding deep embeddings. An online triplet mining approach is then employed on the embeddings to select the triplets consisting of anchor, positive and negative samples. PoreNet then learns the deep embedding representation such that it minimizes the triplet loss. Finally, in verification step, descriptors generated from the PoreNet are compared using the Euclidean distance. Further, the distance ratio d_r is employed to refine the matched descriptor pairs. In the proposed approach, the match score is equal to the number of the matched descriptors between the two fingerprint images. The schematic diagram of the proposed methodology is presented in Fig. 1.

A. Pore label generation

For a given training dataset, we first detect pores present in fingerprint images by employing the DeepResPore model as



(a) Detection of pores in high-resolution fingerprint images using DeepResPore



(b) Pore-based fingerprint matching

Fig. 1. Schematic diagram of the proposed fingerprint recognition approach

shown in Fig. 1(a). DeepResPore generates a pore intensity map for a given input fingerprint image. The pore intensity map is then processed further to obtain the pore coordinates. In order to train a CNN model in a supervised manner, we require a labeled dataset. Specifically, for training PoreNet, we require pore patches and their corresponding labels. Therefore, we first obtain labels of the same pores present in the different impressions of the same fingerprint image.

For generating the pore labels, we have employed a hand-crafted key-point descriptor. As the authors in [26] have presented that Daisy-based descriptor is more efficient in pore representation than the other descriptors. Therefore, in this work, we have employed Daisy-based descriptor for generating the pore labels. The steps involved in pore label generation are as follows: we first obtain the reference fingerprint image for each of the finger present in the training dataset. In order to do so, the detected pore coordinates in a fingerprint image are treated as key-points and then Daisy-based descriptor [27] is obtained for each of the detected pores. For a given finger, we have several impressions in the training dataset. Thus, for a same finger, all its impressions are compared with each other using the Daisy-based descriptor and their match scores (i.e. number of matched descriptors) are stored in a variable M_{score} . Then, the reference image is obtained as :

$$Ref_{img} = \max_r \left\{ \left(\sum_{i=1}^N (M_{score})_i \right)_r \right\} \quad (1)$$

where r is number of impressions of the same finger and N is total number of comparisons made. The impression (r) for which the sum of M_{score} is maximum is considered as the reference image.

Once we have obtained the reference fingerprint image for each finger then the remaining impressions are aligned to

the reference fingerprint to find the common pores present in all the impressions of a finger. Firstly, we find the Daisy-based pore descriptor of the reference and the moving images. Further, the transformation matrix T_M is obtained based on the matched descriptors. Furthermore, T_M is applied on the moving fingerprint image to obtain the transformed image which has overlapping region with the reference image. Next, each pore coordinates in the reference image is matched with the pore coordinates in the other transformed impressions to find the common pores. After completion of this step, we have number of matched pores present in all the impressions of every finger. Finally, a patch of size 41×41 pixels centered at common pore is extracted and given a unique label. It is important to note that a sample finger having P common pores between all its impressions (r) will have $P \times r$ number of pore patches having same label in the training set.

B. Pore descriptor learning

After completion of the pore label generation step, we have pore patches $X = \{x_1, x_2, \dots, x_T\}$ and their corresponding labels $Y = \{y_1, y_2, \dots, y_T\}$ of all the fingerprint images present in the training dataset. For learning a pore patch descriptor, we have designed a customized residual learning-based CNN model referred to as PoreNet. The detailed architecture of PoreNet is presented in Table I. As can be observed, the proposed PoreNet contains 14 learnable layers with 4 residual blocks consisting of a total of 4 shortcut connections. PoreNet takes a pore patch of size 41×41 pixels as input and provide the corresponding pore descriptor of dimension 1681 as output. It is important to note that PoreNet does not perform pooling operation in order to maintain the size of output feature map same as that of the input. At the end of network, we have introduced a convolutional layer containing a single filter to provide the final feature map. The output of which is flattened and L2-normalized to constrain the output descriptor vector in d -dimensional hypersphere, such that l_2 -norm of the output embeddings is equal to one [22]. All convolutional layers in the PoreNet perform convolution with a stride of one. At every stage, zero padding is employed to maintain the size of the feature map. Furthermore, all convolutional layers, except the last one, perform convolution followed by batch normalization [28] and ReLU activation.

During the training phase, the PoreNet is trained from the scratch. We have trained PoreNet model end-to-end in a supervised learning manner with the objective of minimizing the value of the loss function. Specifically, we have employed triplet loss function in our approach. A batch of pore patches are input to PoreNet, which generate the corresponding high-dimensional embeddings. Next, we apply an online triplet mining scheme termed as batch-hard triplet mining on the obtained embeddings. In this method, for each anchor sample (a), we first obtain the hardest positive sample (p) having the same label as that of anchor and the hardest negative sample (n) having different label than the anchor. Finally, we combine them into the triplet loss as follows [22]:

$$L_{triplet} = \max \{d(a, p) - d(a, n) + margin, 0\} \quad (2)$$

where $d(a, p)$ is the distance between the a and p and $d(a, n)$ is the distance between a and n . The PoreNet is trained in an end-to-end manner to minimize the triplet loss. During the test phase output from the PoreNet is treated as the pore descriptor which is used in fingerprint verification task.

TABLE I
DETAILED ARCHITECTURE OF PORENET

Layer name	Output shape	Kernel
conv1	$41 \times 41, 16$	$3 \times 3, 16, \text{stride } 1, \text{padding same}$
conv2_x	$41 \times 41, 64$	$\begin{bmatrix} 1 \times 1, 32 \\ 3 \times 3, 32 \\ 1 \times 1, 64 \end{bmatrix} \times 2$
conv3_x	$41 \times 41, 128$	$\begin{bmatrix} 1 \times 1, 64 \\ 3 \times 3, 64 \\ 1 \times 1, 128 \end{bmatrix} \times 2$
conv4	$41 \times 41, 1$	$3 \times 3, 1$
Flatten	1681	—
L2-norm	1681	—
Total parameters	142,881	—

Once PoreNet is trained, our focus is then to match the fingerprint images using pore patch descriptor. For two fingerprint images I_1 and I_2 containing p_n and p_m pore patches, respectively. PoreNet will generate $P_1 \in \mathbb{R}^{n \times l}$ and $P_2 \in \mathbb{R}^{m \times l}$ pore descriptors, where l is 1681. Pore descriptors in P_1 are then compared with the pore descriptors in P_2 using the Euclidean distance between them. Descriptors satisfying the bi-directional match are retained. Finally the matched descriptors are refined by employing d_r criterion on the second nearest neighbour of each of the matched descriptors [29].

III. EXPERIMENTAL RESULTS AND DISCUSSION

In this section, we first present the dataset preparation for training the PoreNet model followed by the pore matching results obtained from our experiments.

1) *Dataset preparation:* We have performed our experiments on the publicly available PolyU HRF dataset [30] which contains high-resolution fingerprint images of resolution 1200 dpi in two different sets DBI and DBII. DBI contains two subsets: DBI-train dataset which contains 210 (35×6) partial fingerprint images and DBI-test containing 1480 (148×10) partial fingerprint images of size 320×240 pixels. On the other hand, DBII contains 1480 complete fingerprint images of size 640×480 pixels. In order to obating pore patches for training the PoreNet we have used the DBI-train dataset and tested our approach on the DBI-test and DBII datasets following the same experimental protocol set in the previous approaches [15], [19], [21]. We have obtain the train (80%) and validation (20%) sets by randomly partitioning the DBI-train images. From the training set, we obtain the pore patches and their corresponding labels by following the method detailed in Section II-A. Furthermore, we have employed the data augmentation techniques to increase the number of training data. Specifically, we have included ten random rotation between -20° to 20° degrees and ten random translation between -5 to 5 pixels. We have also employed the contrast correction on training data so that the trained network is robust to the contrast variations. Overall, we have generated 891532 labelled pore patches for training.

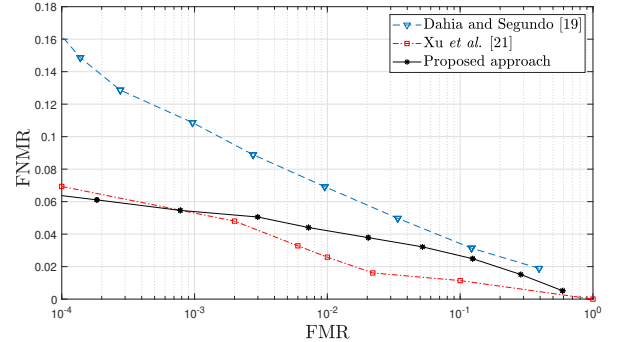
2) *Experimental results*: In our experiments, PoreNet has been trained end-to-end in a supervised manner. Specifically, PoreNet has been trained for 100 epochs using a batch size of 256 and learning rate of 0.0001. We have employed adaptive moment estimation (ADAM) for optimizing the loss function. The margin for the triplet loss function is set to 0.8. All our experiments have been performed on a system with a configuration of 3.60 GHz Intel core i7-6850K processor, 48 GB RAM and Nvidia GTX 1080 8 GB GPU. We have performed our experiments in MATLAB and Python environment. Specifically, pore patch generation part has been performed in MATLAB environment whereas training and testing of PoreNet has been performed in Python environment using TensorFlow [31].

In order to have a fair comparison with the existing approaches, we have followed the same experimental protocol as in [15], [19], [21]. The genuine scores have been obtained by comparing each fingerprint image of the second session with all the fingerprint images of the first session for the same finger. On the other hand, impostor scores have been generated by comparing the first sample from the second session of a finger with the first sample of the first session of all other fingers. Thus, we have a total of 3700 (25×148) genuine scores and 21,756 (148×147) impostor scores. We have employed equal error rate (EER), FMR1000 and FMR10000 [32] as the performance measure for reporting the results. We have also presented the detection error trade-off (DET) curve to ascertain the performance of the proposed approach. The results for this set of experiments on the PolyU datasets are presented in Table II ¹. As can be observed from Table II, the proposed approach provides comparable (with in 0.25% points) EER with the current state-of-the-art approach [21] on DBI and DBII. Specifically, the DET curves for this set of experiments are presented in Fig. 2. As can be observed, the proposed approach provides the lowest FNMR values for FMR values of 10^{-4} and 10^{-3} . Thus, the proposed approach is more user convenient as well as it provides high security. The FMR1000 and FMR10000 values of the existing and the proposed approach are presented in Table III. As can be observed, the proposed approach provides the lowest FMR1000 and FMR10000 values for both the datasets. Specifically, the proposed PoreNet model provides an improvement of 0.5%, 0.77% and 0.5%, 0.35% points in FMR10000 and FMR1000 values over the current state-of-the-art approach on DBI and DBII, respectively. Furthermore, the proposed approach performs the comparison of two given fingerprint images by taking an average time of 1.41 seconds for DBI and 2.80 seconds for DBII as compared to 8.46 seconds taken by [21] Hence, the proposed approach can be employed for real time applications.

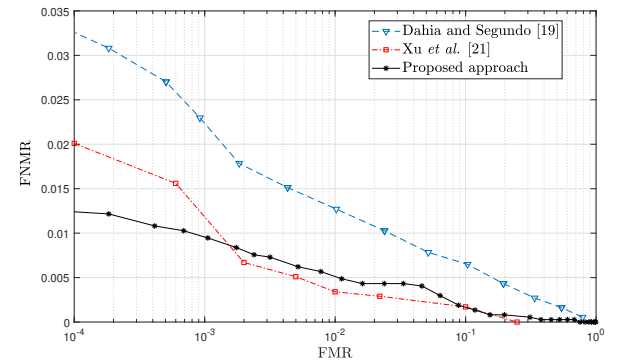
Overall, the experimental results presented in this section indicate that the proposed approach provides a comparable EER with the current state-of-the-art approach [21] on all the datasets. Most importantly, the proposed PoreNet model

TABLE II
EER VALUES ON POLYU DATASETS

Method	EER (%)	
	DBI	DBII
Jain <i>et al.</i> [8]	30.45%	7.83%
Zhao <i>et al.</i> [9]	15.42%	7.05%
Liu <i>et al.</i> [12]	6.59%	0.97%
Liu <i>et al.</i> [13]	3.25%	0.53%
Segundo and Lemes [15]	3.74%	0.76%
Dahia and Segundo [19]	3.05%	0.44%
Xu <i>et al.</i> [21]	1.73%	0.51%
Proposed approach	2.56%	0.57%



(a) DBI



(b) DBII

Fig. 2. DET curves for the proposed approach and the existing approach on PolyU datasets

TABLE III
FMR VALUES FOR EXISTING AND PROPOSED APPROACH

Method	FMR10000		FMR1000	
	DBI	DBII	DBI	DBII
Dahia and Segundo [19]	16.20%	3.33%	10.82%	2.25%
Xu <i>et al.</i> [21]	6.94%	2.01%	5.92%	1.31%
Proposed approach	6.47%	1.24%	5.42%	0.96%

provides lower FMR10000 and FMR1000 values as compared to the current state-of-the-art approach on both the datasets.

IV. CONCLUSION

In this paper, we have presented a methodology for fingerprint recognition using pore-based matching. Specifically, we have developed a residual learning-based CNN named PoreNet

¹The EER values for the existing approaches [8], [9], [12], [15] are directly taken from the results presented in [15] and the EER values for approaches [13] and [21] are taken from [21].

for learning descriptor from pore patches obtained from high-resolution fingerprint images. PoreNet generates deep embeddings from the given fingerprint image. Subsequently, we have also developed a pore label generation methodology which generates the pore label by transforming the images based on the matched pore-based DAISY descriptors and finding the common pore between them. Experiments are performed on the publicly available PolyU datasets. Our experimental results suggest that the proposed PoreNet is very effective in representing pore patches in high-resolution fingerprint images. Our approach provides comparable EER values with the current state-of-the-art approach. Most importantly, the proposed PoreNet model provides an improvement of 0.5%, 0.77% and 0.5%, 0.35% points in FMR10000 and FMR1000 values over the current state-of-the-art approach on DBI and DBII, respectively.

REFERENCES

- [1] D. Maltoni, D. Maio, A. Jain, and S. Prabhakar, *Handbook of fingerprint recognition*. Springer Science & Business Media, 2009.
- [2] D. Zhang, F. Liu, Q. Zhao, G. Lu, and N. Luo, "Selecting a reference high resolution for fingerprint recognition using minutiae and pores," *IEEE Transactions on Instrumentation and Measurement*, vol. 60, no. 3, pp. 863–871, 2011.
- [3] S. Meagher and A. Hicklin, "Extended fingerprint feature set," in *ANSI/NIST IITL 1-2000 Standard Update Workshop*, 2005.
- [4] J. D. Stosz and L. A. Alyea, "Automated system for fingerprint authentication using pores and ridge structure," in *Proc. SPIE*, vol. 2277, 1994, pp. 2277 – 2277 – 14.
- [5] A. R. Roddy and J. D. Stosz, "Fingerprint features-statistical analysis and system performance estimates," *Proc. of the IEEE*, vol. 85, no. 9, pp. 1390–1421, 1997.
- [6] K. Kryszczuk, A. Drygajlo, and P. Morier, "Extraction of level 2 and level 3 features for fragmentary fingerprint," *Second COST Action 275 Workshop*, pp. 83–88, 2004.
- [7] K. M. Kryszczuk, P. Morier, and A. Drygajlo, "Study of the distinctiveness of level 2 and level 3 features in fragmentary fingerprint comparison," in *Biometric Authentication*. Springer, 2004, pp. 124–133.
- [8] A. K. Jain, Y. Chen, and M. Demirkus, "Pores and ridges: high-resolution fingerprint matching using level 3 features," *IEEE Trans Pattern Anal. Mach. Intell.*, vol. 29, no. 1, pp. 15–27, Jan 2007.
- [9] Q. Zhao, L. Zhang, D. Zhang, and N. Luo, "Direct pore matching for fingerprint recognition," in *Advances in Biometrics*. Springer, 2009, pp. 597–606.
- [10] Q. Zhao, D. Zhang, L. Zhang, and N. Luo, "Adaptive fingerprint pore modeling and extraction," *Pattern Recognit.*, vol. 43, no. 8, pp. 2833 – 2844, 2010.
- [11] —, "High resolution partial fingerprint alignment using "porevalley" descriptors," *Pattern Recognition*, vol. 43, no. 3, pp. 1050 – 1061, 2010.
- [12] F. Liu, Q. Zhao, L. Zhang, and D. Zhang, "Fingerprint pore matching based on sparse representation," in *20th International Conference on Pattern Recognition*, Aug 2010, pp. 1630–1633.
- [13] F. Liu, Q. Zhao, and D. Zhang, "A novel hierarchical fingerprint matching approach," *Pattern Recognition*, vol. 44, no. 8, pp. 1604 – 1613, 2011.
- [14] R. d. P. Lemes, M. P. Segundo, O. R. P. Bellon, and L. Silva, "Dynamic pore filtering for keypoint detection applied to newborn authentication," *Proc. Int. Conf. on Pattern Recognition (ICPR)*, pp. 1698–1703, Aug 2014.
- [15] M. P. Segundo and R. d. P. Lemes, "Pore-based ridge reconstruction for fingerprint recognition," in *Proc. IEEE Conf. on Computer Vision and Pattern Recognition Workshops (CVPRW)*, 2015, pp. 128–133.
- [16] V. Anand and V. Kanhangad, "Pore based indexing for high-resolution fingerprints," in *IEEE International Conference on Identity, Security and Behavior Analysis (ISBA)*, Feb 2017, pp. 1–6.
- [17] Q. Zhao, L. Zhang, D. Zhang, N. Luo, and J. Bao, "Adaptive pore model for fingerprint pore extraction," in *2008 19th International Conference on Pattern Recognition*, Dec 2008, pp. 1–4.
- [18] D. Zhang, W. Wang, Q. Huang, S. Jiang, and W. Gao, "Matching images more efficiently with local descriptors," in *19th International Conference on Pattern Recognition*, Dec 2008, pp. 1–4.
- [19] G. Dahia and M. P. Segundo, "Automatic dataset annotation to learn cnn pore description for fingerprint recognition," *CoRR*, vol. abs/1809.10229, 2018. [Online]. Available: <http://arxiv.org/abs/1809.10229>
- [20] A. Mishchuk, D. Mishkin, F. Radenovic, and J. Matas, "Working hard to know your neighbor's margins: Local descriptor learning loss," in *Proceedings of NIPS*, Dec. 2017, pp. 4826–4837.
- [21] Y. Xu, G. Lu, Y. Lu, F. Liu, and D. Zhang, "Fingerprint pore comparison using local features and spatial relations," *IEEE Transactions on Circuits and Systems for Video Technology*, 2018, "early access".
- [22] F. Schroff, D. Kalenichenko, and J. Philbin, "Facenet: A unified embedding for face recognition and clustering," in *IEEE Conference on Computer Vision and Pattern Recognition (CVPR)*, June 2015, pp. 815–823.
- [23] O. M. Parkhi, A. Vedaldi, and A. Zisserman, "Deep face recognition," in *Proceedings of the British Machine Vision Conference (BMVC)*. BMVA Press, September 2015, pp. 41.1–41.12.
- [24] E. Simo-Serra, E. Trulls, L. Ferraz, I. Kokkinos, P. Fua, and F. Moreno-Noguer, "Discriminative learning of deep convolutional feature point descriptors," in *IEEE International Conference on Computer Vision (ICCV)*, Dec 2015, pp. 118–126.
- [25] V. Anand and V. Kanhangad, "Pore detection in high-resolution fingerprint images using deep residual network," *Journal of Electronic Imaging*, vol. 28, no. 2, pp. 1 – 4 – 4, 2019.
- [26] —, "Pore-based indexing for fingerprints acquired using high-resolution sensors," *Pattern Analysis and Applications*, Mar 2019.
- [27] E. Tola, V. Lepetit, and P. Fua, "A fast local descriptor for dense matching," in *IEEE Conference on Computer Vision and Pattern Recognition*, June 2008, pp. 1–8.
- [28] S. Ioffe and C. Szegedy, "Batch normalization: Accelerating deep network training by reducing internal covariate shift," *CoRR*, vol. abs/1502.03167, 2015.
- [29] D. G. Lowe, "Distinctive image features from scale-invariant keypoints," *Int. J. Comput. Vision*, vol. 60, no. 2, pp. 91–110, Nov. 2004.
- [30] "PolyU HRF Database," Hong kong, 2009, http://www4.comp.polyu.edu.hk/~biometrics/HRF/HRF_old.htm.
- [31] M. Abadi, P. Barham, J. Chen, Z. Chen, A. Davis, J. Dean, M. Devin, S. Ghemawat, G. Irving, M. Isard, M. Kudlur, J. Levenberg, R. Monga, S. Moore, D. G. Murray, B. Steiner, P. Tucker, V. Vasudevan, P. Warden, M. Wicke, Y. Yu, and X. Zheng, "Tensorflow: A system for large-scale machine learning," in *12th USENIX Symposium on Operating Systems Design and Implementation (OSDI 16)*, 2016, pp. 265–283.
- [32] R. Cappelli, M. Ferrara, D. Maltoni, and F. Turrone, "Fingerprint verification competition at ijcb2011," in *International Joint Conference on Biometrics (IJCB)*, Oct 2011, pp. 1–6.